

Northern Hemisphere glaciation and the evolution of Plio-Pleistocene climate noise

Stephen R. Meyers¹ and Linda A. Hinnov²

Received 29 July 2009; revised 3 December 2009; accepted 20 January 2010; published 4 August 2010.

[1] Deterministic orbital controls on climate variability are commonly inferred to dominate across timescales of 10^4 – 10^6 years, although some studies have suggested that stochastic processes may be of equal or greater importance. Here we explicitly quantify changes in deterministic orbital processes (forcing and/or pacing) versus stochastic climate processes during the Plio-Pleistocene, via time-frequency analysis of two prominent foraminifera oxygen isotopic stacks. Our results indicate that development of the Northern Hemisphere ice sheet is paralleled by an overall amplification of both deterministic and stochastic climate energy, but their relative dominance is variable. The progression from a more stochastic early Pliocene to a strongly deterministic late Pleistocene is primarily accommodated during two transitory phases of Northern Hemisphere ice sheet growth. This long-term trend is punctuated by “stochastic events,” which we interpret as evidence for abrupt reorganization of the climate system at the initiation and termination of the mid-Pleistocene transition and at the onset of Northern Hemisphere glaciation. In addition to highlighting a complex interplay between deterministic and stochastic climate change during the Plio-Pleistocene, our results support an early onset for Northern Hemisphere glaciation (between 3.5 and 3.7 Ma) and reveal some new characteristics of the orbital signal response, such as the puzzling emergence of 100 ka and 400 ka cyclic climate variability during theoretical eccentricity nodes.

Citation: Meyers, S. R., and L. A. Hinnov (2010), Northern Hemisphere glaciation and the evolution of Plio-Pleistocene climate noise, *Paleoceanography*, 25, PA3207, doi:10.1029/2009PA001834.

1. Introduction

[2] Global climate change occurs on multiple time scales [Mitchell, 1976], characterized by the interplay of rhythmic variability, long-term trends, as well as more abrupt events or transitions [Zachos *et al.*, 2001]. A paramount objective of paleoclimatology is the deconvolution of these modes of variability, and their assignment to specific climate forcing mechanisms. At the heart of this endeavor lies a fundamental debate about the relative role of deterministic versus stochastic controls on climate. For example, orbital climate theory provides a powerful deterministic framework for the analysis of rhythmic climate change on timescales of 10^4 – 10^6 years, and has become a cornerstone of paleoclimatology [e.g., Milankovitch, 1941; Hays *et al.*, 1976; Hinnov, 2000; Zachos *et al.*, 2001; Lourens *et al.*, 2005; Pälike *et al.*, 2006; Pälike and Hilgen, 2008]. On these timescales, the stochastic component of climate has received less attention, although some studies argue for the dominance of stochastic processes [Hasselmann, 1976; Lorenz, 1976; Kominz and Pisias, 1979; Saltzman, 1982; Pelletier, 1998, 2002, 2003; Wunsch, 2003, 2004]. Clearly, a complete

understanding of the controls on climate change necessitates an assessment of both deterministic and stochastic processes, potential linkages between the two [Benzi *et al.*, 1983; Ganopolski and Rahmstorf, 2002; Huybers and Curry, 2006; Ditlevsen, 2009], and their evolution with Earth’s mean climate state.

[3] In this study, we provide the first explicit and comprehensive evaluation of temporal changes in deterministic orbital processes (forcing and/or pacing [Hays *et al.*, 1976; Imbrie *et al.*, 1992, 1993]) versus stochastic climate processes during the Plio-Pleistocene epochs (please note that we utilize updated definitions of the Pliocene (5.332 Ma–2.588 Ma) and Pleistocene (2.588 Ma–0.0117 Ma), as proposed by the International Commission on Stratigraphy, and ratified by the International Union of Geological Sciences (June 29, 2009)). Our analysis evaluates two prominent marine oxygen isotope stacks that have become staples of the paleoclimate community [Lisiecki and Raymo, 2005; Huybers, 2007], with a specific focus on the 1/10,000 to 1/500,000 yr^{-1} frequency band. Quantification of the relative influence of orbital versus stochastic climate variability in such proxy records has historically proven challenging, and as a consequence, many studies have adopted strict ideological stances for or against deterministic orbital influence, especially in deep time strata. Complicating this issue, the philosophical distinction between stochastic and deterministic climate processes is not always obvious. For example, consider the fact that the stochastic component of climate ultimately derives from deterministic phenomena

¹Department of Geoscience, University of Wisconsin-Madison, Madison, Wisconsin, USA.

²Morton K. Blaustein Department of Earth and Planetary Sciences, Johns Hopkins University, Baltimore, Maryland, USA.

(e.g., equations of motion). However, of critical importance, stochastic phenomena lack a simple phase coherence with their primary forcing (e.g., the annual cycle, orbital forcing, etc.).

[4] The loss of phase coherence between primary forcing and observed stochastic climate variability is attributable to a myriad of complex interactions within the climate system. To simulate this physical complexity, stochastic climate variability is often treated as a simple autoregressive [Hasselmann, 1976] or fractional Gaussian noise process [Pelletier and Turcotte, 1997], models that are physically analogous to weather persistence. Such stochastic noise models are characterized by relatively smooth power spectra, also known as the spectral “continuum,” and thus the spectral continuum observed in climate proxy data has often been used as a measure of the stochastic component of climate change [e.g., Pelletier, 1998; Wunsch, 2003, 2004]. To further illustrate the complexity of this issue, deterministic controls on weather and climate (the annual cycle and orbital forcing) have been demonstrated to exert substantial control on the “stochastic” spectral continuum [Huybers and Curry, 2006].

[5] Given these philosophical complications it is necessary to adopt a very strict definition of the deterministic climate change that we seek to evaluate in this study. Herein we are primarily concerned with a subset of deterministic processes, that is, phase-coherent periodic signals in the orbital bands. There are many other potential deterministic forcing factors that influence climate, such as geophysical changes in ice sheet dynamics [Clark and Pollard, 1998; Clark et al., 1999], the opening and closing of oceanic gateways [Keigwin, 1982; Haug and Tiedemann, 1998; Zachos et al., 2001; Cane and Molnar, 2001; Lawver and Gahagan, 2003], and long-term changes in the global carbon cycle [Pearson and Palmer, 2000; Berner and Kothavala, 2001; Pagani et al., 2005; Royer, 2006; Hönisch et al., 2009]. Although these nonorbital climate forcings are not explicitly evaluated in our statistical approach (see section 2), we will demonstrate that they can be assessed, in an indirect manner, through their influence on phase-coherent climate response within the orbital bands, as well through as their influence on the character of the stochastic continuum.

[6] As discussed in detail below, our analysis reveals large and sometimes abrupt changes in the relative dominance of stochastic versus deterministic energy, as well as in the character of the stochastic continuum. These changes parallel the evolution of the Plio-Pleistocene climate system, and more specifically, the development of Northern Hemisphere glaciation. This analysis also reveals some important, and previously undocumented, characteristics of the orbital signal response, and demonstrates variable linkages between stochastic and deterministic climate processes during the Plio-Pleistocene.

2. Data and Methodology

[7] Our analysis of deterministic versus stochastic climate variability during the Plio-Pleistocene focuses on two well-studied climate proxy records. The first of these is the

benthic foraminifera oxygen isotope stack of *Lisiecki and Raymo* [2005, hereafter LR04] (obtained from <http://lorraine-lisiecki.com/LR04stack.txt>), which spans 0–5.32 Ma. This time series provides a robust globally integrated record of changes in deep ocean temperature and ice sheet size [Shackleton, 2000; Bintanja and van de Wal, 2008]. Of important note, the LR04 stack has been tuned using a simple ice sheet model driven by insolation received at 65°N on 21 June [Imbrie and Imbrie, 1980], and thus presumes a strong deterministic orbital control on climate [Lisiecki and Raymo, 2005].

[8] We supplement this analysis with an assessment of the planktic/benthic foraminifera oxygen isotope stack of *Huybers* [2007, hereafter H07] (obtained from <http://www.people.fas.harvard.edu/~phuybers/Progression/Averages.txt>), which spans 0–2.58 Ma. Importantly, the H07 stack has been tuned using a “depth-derived” time scale approach [Huybers and Wunsch, 2004; Huybers, 2007], and thus does not presume a strong orbital influence on climate. In our analyses, the LR04 and H07 oxygen isotope stacks provide end-member conditions for evaluation of the sensitivity of climate change to deterministic and stochastic processes.

[9] The LR04 and H07 stacks are investigated using a statistical methodology that is specifically designed to separate deterministic periodic signals (phase-coherent sinusoids; the spectral “lines”) from the spectral continuum. Following the approach of previous studies [e.g., Pelletier, 1998; Wunsch, 2003, 2004], we utilize the spectral continuum as a measure of stochastic variability. The complete technique, attributable to *Thomson* [1982] and known as the multitaper method (MTM), has been previously applied to the Vostok temperature series to assess the importance of orbital forcing/pacing and stochastic variability in late Pleistocene climate change [Meyers et al., 2008]. Detailed descriptions of the procedures utilized herein can be found in the work by *Thomson* [1982], *Mann and Lees* [1996], *Percival and Walden* [1993], and *Meyers et al.* [2001, 2008]. To examine the temporal evolution of the stochastic and deterministic components of climate, a MTM time-frequency approach is implemented [e.g., *Park and Herbert*, 1987; *Yiou et al.*, 1991; *Meyers et al.*, 2001].

3. Analysis of Deterministic and Stochastic Climate Change During the Plio-Pleistocene: LR04 Stack

[10] To begin, evolutive harmonic analysis (EHA) [Meyers et al., 2001] is applied to identify and quantify statistically significant periodic components in the LR04 stack, using a 500 ka moving window (Figure 1). To assist in visualization of the results, two operations are performed on the raw EHA amplitude spectra in Figure 1b. First, each amplitude spectrum is normalized so that it has a maximum amplitude of unity (see also Figure S1), to better illustrate changes in the dominance of individual periodic signals throughout the study interval.¹ Second, these results are filtered at the 90% significance level to isolate those

¹Auxiliary materials are available in the HTML. doi:10.1029/2009PA001834.

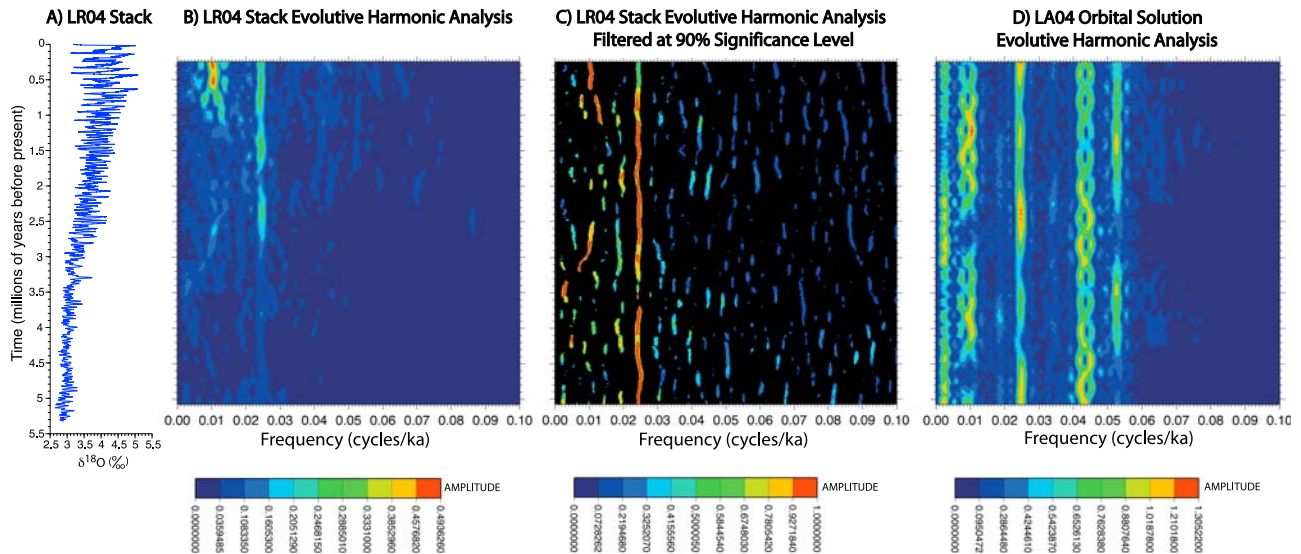


Figure 1. MTM evulsive harmonic analysis results for the LR04 stack. All EHA computations were conducted using three 2π prolate tapers and a 500 ka moving window with a 5 ka increment. The mean value and a linear trend have been removed from each 500 ka data window prior to analysis. (a) The LR04 stack. (b) EHA amplitude results for the LR04 stack. (c) EHA amplitude results in Figure 1b, normalized so that each individual spectrum has a maximum amplitude of unity (see Figure S1) and filtered at the 90% significance level to isolate frequency components with a strong periodic character. Frequencies below the 90% significance level are indicated in black. (d) EHA amplitude results for the *Laskar et al.* [2004] normalized eccentricity-tilt-precession series (ETP). Following removal of the mean value from the eccentricity, tilt, and precession solutions, each component was divided by its respective standard deviation and finally added to construct the normalized ETP series.

frequency components that show a strong periodic (phase-coherent) character. Our analysis identifies the expected strong 41 ka obliquity component, and the well-known shift to a dominant “100,000” cycle over the past ~ 1.2 million years. In contrast, precession periods are not as well resolved in the LR04 stack.

[11] Comparison of the LR04 stack results (Figure 1c) to the theoretical orbital solution of *Laskar et al.* [2004, hereafter LA04] (Figure 1d) reveals new insights into the evolution of low frequency Plio-Pleistocene climate change. A short-lived interval with strong 100 ka periodic $\delta^{18}\text{O}$ variability is observed in the LR04 data centered at ~ 2.75 Ma (Figures 1c and 2b), and surprisingly, it is associated with a lull (“node”) in the LA04 theoretical short eccentricity signal (Figures 1d and 2a). In addition, an interval dominated by 400 ka periodic $\delta^{18}\text{O}$ variability is observed in the LR04 data centered at ~ 3.5 Ma (Figures 1c and 2d), and this interval is associated with a node in the LA04 theoretical long eccentricity signal (Figures 1d and 2c). The recent interval of 100 ka cyclic $\delta^{18}\text{O}$ variability (most clearly expressed 600 Ka to present) is also associated with a relatively diminished theoretical short eccentricity variability. The nearly exclusive occurrence of high amplitude 100 ka and 400 ka $\delta^{18}\text{O}$ cycles during their respective theoretical eccentricity nodes suggests some linkage to an orbital signal, although clearly not by direct amplification of eccen-

tricity changes. This topic will be considered further in section 5.

[12] Having identified the periodic components and their evolution throughout the Plio-Pleistocene, we can now turn to an analysis of the stochastic continuum. Figure 3b displays a MTM evulsive power spectral analysis (EPSA) of the LR04 stack, using a 500 ka moving window (note, each spectrum is normalized such that total power is equivalent to the total data variance in each 500 ka window). These EPSA results include power from both the periodic components (Figure 1c) and the stochastic continuum. In Figure 3c, the power attributable to the statistically significant periodic components has been removed. This residual power constitutes the stochastic continuum (also termed reshaped spectrum, or reshaped continuum). The reshaped EPSA results indicate that observed low frequency climate variability (i.e., 100 ka and 400 ka) is not exclusively deterministic or stochastic. Rather, variability at these timescales contains substantial energy associated with both deterministic and stochastic sources (see the residual stochastic power in Figure 3c). In contrast, most of the obliquity band and precession band energy appears to be deterministic. We can conclude that evolution of the Plio-Pleistocene climate system is paralleled by an overall enhancement of low frequency stochastic variability, the onset of which occurs by at least 3.5 Ma.

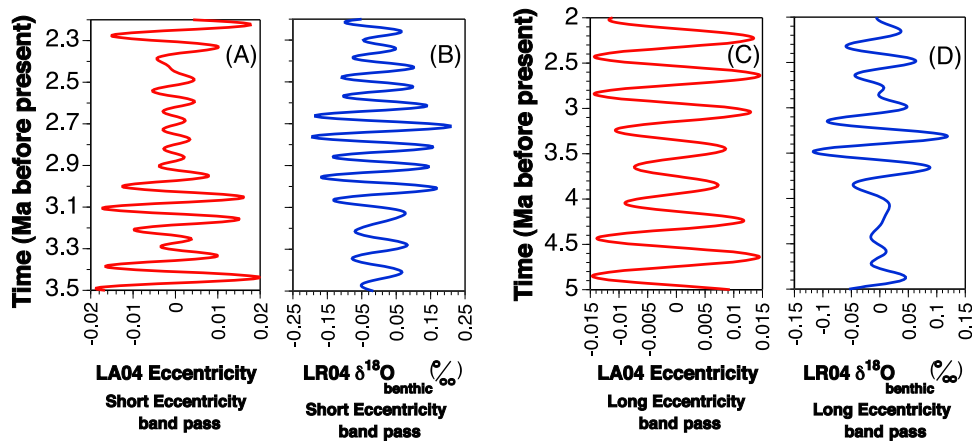


Figure 2. Band-pass filtered records, which illustrate the occurrence of high amplitude 100 ka and 400 ka $\delta^{18}\text{O}$ cycles in the LR04 stack, contemporaneous with nodes in the LA04 theoretical eccentricity. (a) The LA04 orbital solution for eccentricity, filtered to extract short eccentricity band variability using a 10% cosine window with a bandwidth spanning 1/87 ka–1/154 ka. (b) The LR04 stack, filtered to extract short eccentricity band variability using a 10% cosine window with a bandwidth spanning 1/87 ka–1/154 ka. (c) The LA04 orbital solution for eccentricity, filtered to extract long eccentricity band variability using a 10% cosine window with a bandwidth spanning 1/250 ka–1/588 ka. (d) The LR04 stack, filtered to extract long eccentricity band variability using a 10% cosine window with a bandwidth spanning 1/250 ka–1/588 ka.

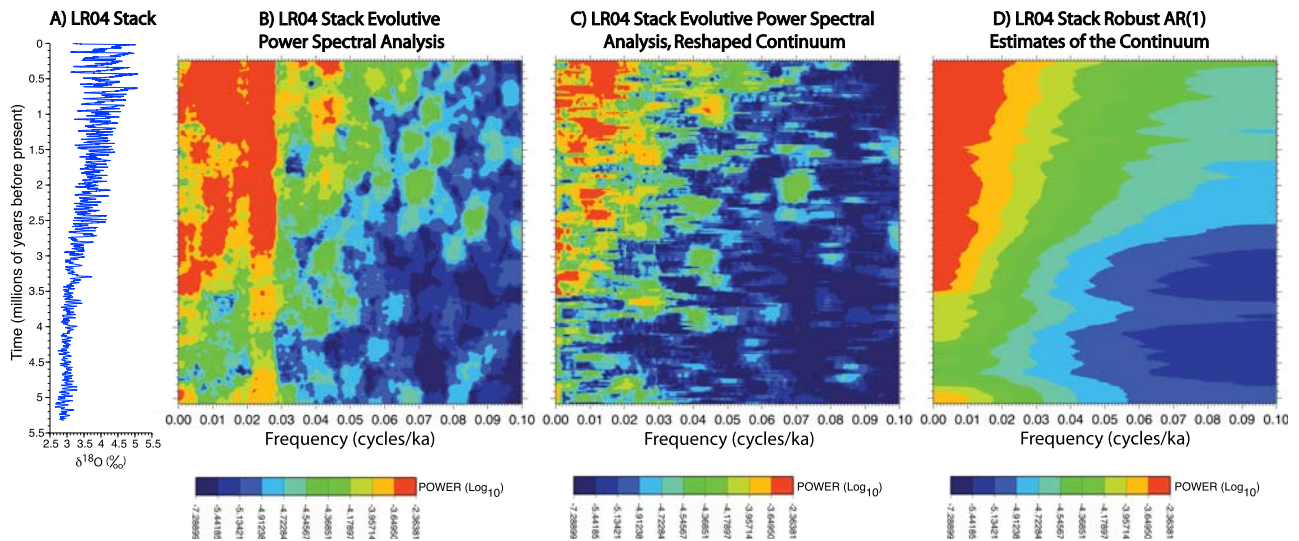


Figure 3. MTM evulsive power spectral analysis results for the LR04 stack. All EPSA computations were conducted using three 2π prolate tapers and a 500 ka moving window with a 5 ka increment. The mean value has been removed from each 500 ka data window prior to analysis. (a) The LR04 stack. (b) Total power (deterministic lines plus stochastic continuum) for the LR04 stack. (c) Reshaped continuum for the LR04 stack, determined by removing the power attributable to the statistically significant periodic components identified in Figure 1c. (d) Autoregressive estimates of the LR04 stack continuum, calculated by fitting a robust AR(1) model [Mann and Lees, 1996] to the power spectra in Figure 3b. Note that the robust red noise algorithm employed in this study does not utilize spectrum reshaping [Meyers et al., 2008], in contrast to Mann and Lees [1996]. Thus, the continuum estimates in Figures 3c and 3d are essentially independent.

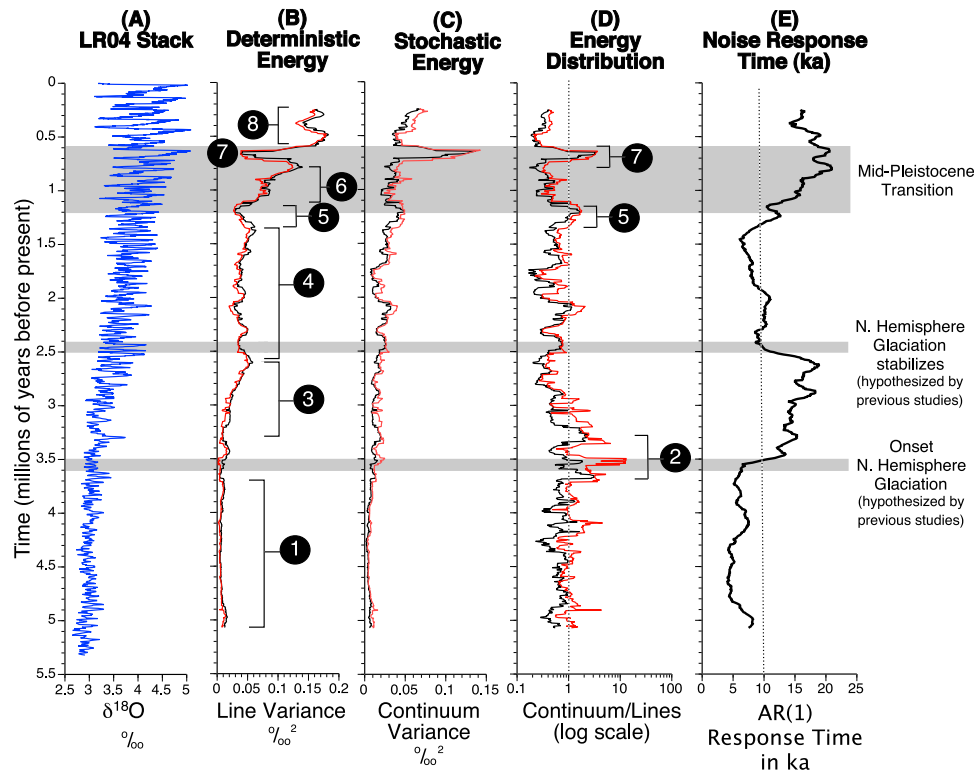


Figure 4. Analysis of the deterministic and stochastic components of climate in the LR04 benthic foraminifera oxygen isotopic stack. (a) The LR04 stack. (b) Evolution of the deterministic line energy observed in the LR04 stack. (c) Evolution of the stochastic energy observed in the LR04 stack. (d) The ratio of stochastic to deterministic energy. Values greater than one indicate dominance of stochastic energy. (e) Noise response time as determined from the robust AR(1) noise models in Figure 3d. The “noise time constant,” which represents the e-folding time for noise decorrelation [Bartlett, 1966], has been converted to an equivalent climate system response time (the time required for 50% of the climate response to be observed). The black lines in Figures 4b, 4c, and 4d were determined using a 90% significance level threshold for the identification of periodic components, and the red lines employ a more conservative 95% significance level.

[13] Assessment of the total climate energy attributable to stochastic processes versus deterministic orbital processes is determined by integration of the “raw” (Figure 3b) and reshaped spectra (Figure 3c), and comparison of these results. A summary of the analysis is displayed in Figure 4, in which we define eight distinct climate intervals.

[14] 1. The first is a stable interval (5.32–3.7 Ma) with respect to total deterministic energy (Figure 4b) and total stochastic energy (Figure 4c). The relative importance of stochastic versus deterministic processes is variable, but on average they contribute almost equally to total climate energy (Figure 4d). This interval predates the inception of Northern Hemisphere ice sheets.

[15] 2. There is an abrupt switch to strong dominance of stochastic climate energy (Figure 4d) at ~3.7 Ma. This approximately coincides with previous estimates for the onset of Northern Hemisphere glaciation [Kleiven *et al.*, 2002; Mudelsee and Raymo, 2005]. The ratio of stochastic energy to deterministic energy in this interval is the highest in the entire record.

[16] 3. A more gradual increase in deterministic climate energy (Figure 4b), as well as its relative importance (Figure 4d), occurs associated with the growth of the Northern Hemisphere ice sheets [Mudelsee and Raymo, 2005]. By 2.8 Ma, the climate system is strongly dominated by deterministic climate change.

[17] 4. The fourth is a relatively stable interval (2.6–1.3 Ma) in terms of total deterministic energy (Figure 4b), also primarily dominated by deterministic climate change (Figure 4d).

[18] 5. There is a rapid drop in deterministic climate energy (Figure 4b) and a clear switch to the dominance of stochastic climate energy (Figure 4d) at ~1.2 Ma. This coincides with the initiation of the mid-Pleistocene transition (MPT) [Clark *et al.*, 2006].

[19] 6. A gradual increase in total deterministic energy (Figure 4b) occurs during the progression of the mid-Pleistocene transition, along with a return to the dominance of deterministic climate energy (Figure 4d).

[20] 7. A rapid drop in total deterministic energy takes place at the end of the mid-Pleistocene transition (~0.7 Ma [Clark *et al.*, 2006]) (Figure 4b), in tandem with a rapid increase in total stochastic energy (Figure 4c), and a temporary switch to domination by stochastic processes.

[21] 8. A late Pleistocene interval (0.6 Ma to present) is strongly dominated by deterministic energy (Figures 4b and 4d).

[22] In summary, our analysis indicates large and sometimes abrupt changes in the relative dominance of stochastic versus deterministic climate energy. The evolution of the Plio-Pleistocene climate system is paralleled by an overall amplification of both deterministic and stochastic climate energy (Figures 4b and 4c) but their relative dominance is variable (Figure 4d). The progression from a more stochastic early Pliocene, to a strongly deterministic late Pleistocene, is primarily accommodated during two transitory phases of Northern Hemisphere ice sheet growth. This long-term history is punctuated by short-lived intervals dominated by stochastic climate energy, which we term “stochastic events.” The observed stochastic events appear to provide the first clear documentation of abrupt reorganization of the climate system as it enters and exits the mid-Pleistocene transition, and at the onset of Northern Hemisphere glaciation.

[23] As a final component of our analysis of the LR04 stack, we investigate the character of the stochastic energy by fitting a robust AR(1) model [Mann and Lees, 1996] to each of the EPSA results in Figure 3b (Figure 3d). This yields an estimate of the stochastic continuum that is much smoother than (and also essentially independent of) the reshaped spectra in Figure 3c. The robust AR(1) model confirms our conclusion about progressive enhancement of low frequency stochastic variability during the evolution of the Plio-Pleistocene climate system. These AR(1) results also provide an estimate of changes in the “noise time constant” [Bartlett, 1966], which indicates the decorrelation time for the noise. This parameter can be compared to the response time associated with individual climate system components (e.g., the amount of time required for 50% of a climate response to be observed in an ice sheet), and thus should yield information about the noise source.

[24] The first marked increase in noise response time occurs at ~3.5 Ma (Figure 4e), approximately coincident with the proposed onset of Northern Hemisphere glaciation [Kleiven *et al.*, 2002; Mudelsee and Raymo, 2005]. This increase in noise response time from 5.1 ka at 3.73 Ma, to 19 ka by 2.62 Ma, suggests the emergence of a new climate system component with a relatively long memory. Our result is consistent with the early onset of Northern Hemisphere ice sheet growth, and its progressive expansion until 2.62 Ma [Mudelsee and Raymo, 2005]. A decrease in the noise response time occurs from 2.62 to 2.41 Ma, and it remains low until the mid-Pleistocene transition. During the MPT, the noise response time increases to its largest value of 21 ka, associated with the establishment of exceptionally large ice sheets in the Northern Hemisphere [Clark *et al.*, 2006]. Thus, changes in the noise response time identify the major phases of growth associated with the Northern Hemisphere ice sheets, and also agree with our inferences

about ice sheet development based on the partitioning of deterministic and stochastic energy (Figures 4b, 4c, and 4d).

[25] The occurrence of elevated AR(1) response times during active ice sheet expansion is possibly due to a change in the relative influence of deep ocean temperature versus ice volume components on the benthic foraminifera $\delta^{18}\text{O}$ record. We hypothesize that during times of active ice sheet expansion, the $\delta^{18}\text{O}$ signal is more strongly imparted with an ice volume signal, yielding a noise response time more characteristic of ice sheets. If this hypothesis is true, it may be possible to deconvolve the ice volume and deep ocean temperature signals, an important objective that has generally proven challenging (however, see Shackleton [2000] and Bintanja and van de Wal [2008]).

4. Analysis of Deterministic and Stochastic Climate Change During the Pleistocene: H07 Stack

[26] To supplement our analysis of the LR04 stack, the analytical approach utilized in section 3 is applied to the shorter H07 stack [Huybers, 2007]. Analysis of this record allows us to independently test the climate history observed in LR04 stack spanning 0–2.58 Ma (see Figure 4). Importantly, this permits an evaluation of the impact of orbital tuning (present in the LR04 stack) on the observed climate change. Results of the H07 analysis are presented in Figures 5, 6, and 7, and are summarized here with an emphasis on evaluating the robustness of the climate history outlined in Figure 4.

[27] The general pattern of energy distribution is remarkably similar between the H07 and LR04 stacks, with a primary difference being the overall amplification of stochastic climate energy in H07, most prominently in the early Pleistocene (compare Figures 4 and 7). The reason for this discrepancy is apparent in the H07 EHA results (Figures 5c and 5d), which demonstrate progressive degradation of the obliquity component beyond 1.5 Ma (also compare with Figure S1). The spectral signature observed in the oldest portion of the H07 stack reveals an increase in the number of high-amplitude harmonic signals, with a scattered distribution, and is consistent with timescale distortion in this portion of the record [Meyers *et al.*, 2001]. This hypothesis is in agreement with uncertainty estimates associated with the H07 stack, which achieve maximum values of up to 15.8 ka (± 1 standard deviation) in the oldest portion of the record [Huybers, 2007]. An alternative hypothesis is that the climate system progressively transitioned from a complex multiharmonic response in the region of the obliquity band, to a response that locks in faithfully to ~40 ka obliquity variability by 1.5 Ma.

[28] Perhaps the most striking feature of the H07 stack analysis is the occurrence of at least five very large stochastic events (Figure 7). Importantly, all of the stochastic events identified in the LR04 stack spanning 0–2.58 Ma are also present in the H07 stack, although they are further amplified in the latter. The H07 results also display a greater sensitivity to the significance level threshold used to identify periodic components (compare the 90% versus 95% significance levels in Figure 7). This sensitivity is the consequence of an overall lower phase coherence in the H07 stack,

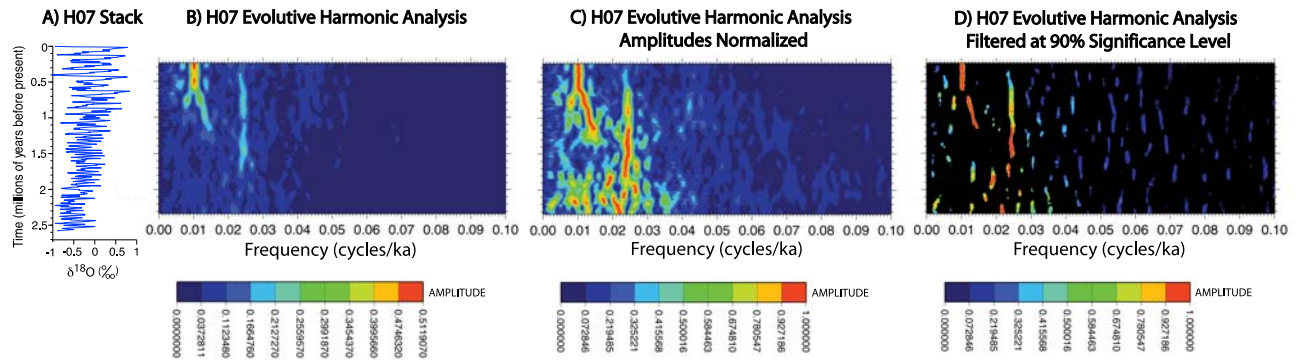


Figure 5. MTM evolutive harmonic analysis results for the H07 stack. All EHA computations were conducted using three 2π prolate tapers and a 500 ka moving window with a 5 ka increment. The mean value and a linear trend have been removed from each 500 ka data window prior to analysis. (a) The H07 stack. Following the convention of *Huybers* [2007], the mean $\delta^{18}\text{O}$ value between 700 and 0 ka is removed. (b) EHA amplitude results for the H07 stack. (c) EHA amplitude results in Figure 5b, normalized so that each individual spectrum has a maximum amplitude of unity. (d) EHA amplitude results in Figure 5c, filtered at the 90% significance level to isolate frequency components with a strong periodic character. Frequencies below the 90% significance level are indicated in black.

which is consistent with a greater degree of timescale error. Furthermore, the stochastic events at ~ 2 Ma and ~ 1.6 Ma in the H07 stack (see the 95% significance level results in Figure 7), which are not observed in the LR04 stack analysis, occur in the vicinity of extreme minima in the LA04 theoretical eccentricity solution. These two LA04 minima are associated with the 400 ka long eccentricity cycle. The concurrence of eccentricity minima and stochastic events at ~ 2 Ma and ~ 1.6 Ma suggests that these events could be artifacts of eccentricity-modulated sedimentation rate changes [*Herbert, 1997; Meyers et al., 2001*] that are not

corrected for in the H07 timescale, but are accounted for in the LR04 stack. In addition, the stochastic events at ~ 2 Ma and ~ 1.6 Ma occur within the two most poorly constrained intervals of the H07 time scale [*Huybers, 2007*], further supporting their spurious nature.

[29] Finally, the robust AR(1) models derived from the H07 stack analysis indicate a subtle enhancement of low frequency stochastic climate variability during the Pleistocene (Figure 6d), broadly consistent with the results from the spectral reshaping (Figure 6c). Noise response times for the H07 stack (Figure 7e) show a similar pattern of evolu-

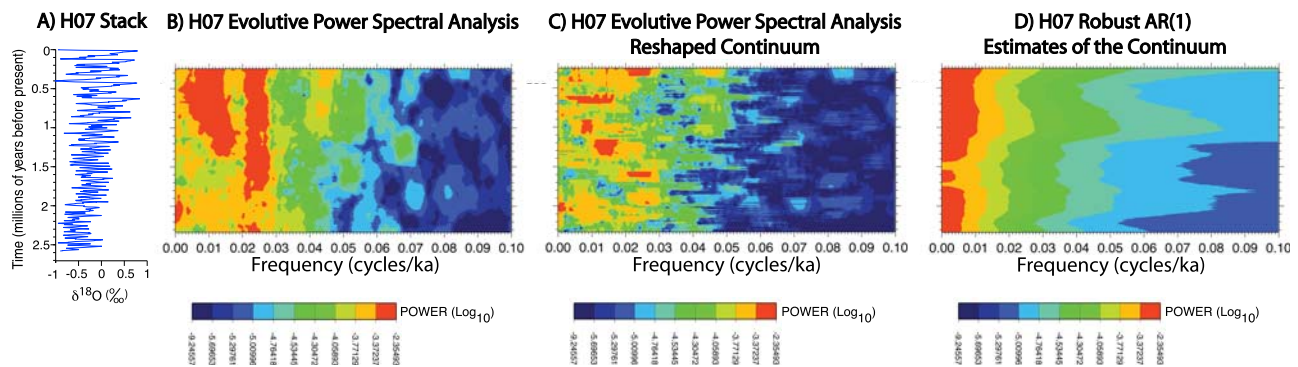


Figure 6. MTM evolutive power spectral analysis results for the H07 stack. All EPSA computations were conducted using three 2π prolate tapers and a 500 ka moving window with a 5 ka increment. The mean value has been removed from each 500 ka data window prior to analysis. (a) The H07 stack. Following the convention of *Huybers* [2007], the mean $\delta^{18}\text{O}$ value between 700 and 0 ka is removed. (b) Total power (deterministic lines plus stochastic continuum) for the H07 stack. (c) Reshaped continuum for the H07 stack, determined by removing the power attributable to the statistically significant periodic components identified in Figure 5d. (d) Autoregressive estimates of the H07 stack continuum, calculated by fitting a robust AR(1) model [*Mann and Lees, 1996*] to the power spectra in Figure 6b. Note that the robust red noise algorithm employed in this study does not utilize spectrum reshaping [*Meyers et al., 2008*], in contrast to *Mann and Lees* [1996]. Thus, the continuum estimates in Figures 6c and 6d are essentially independent.

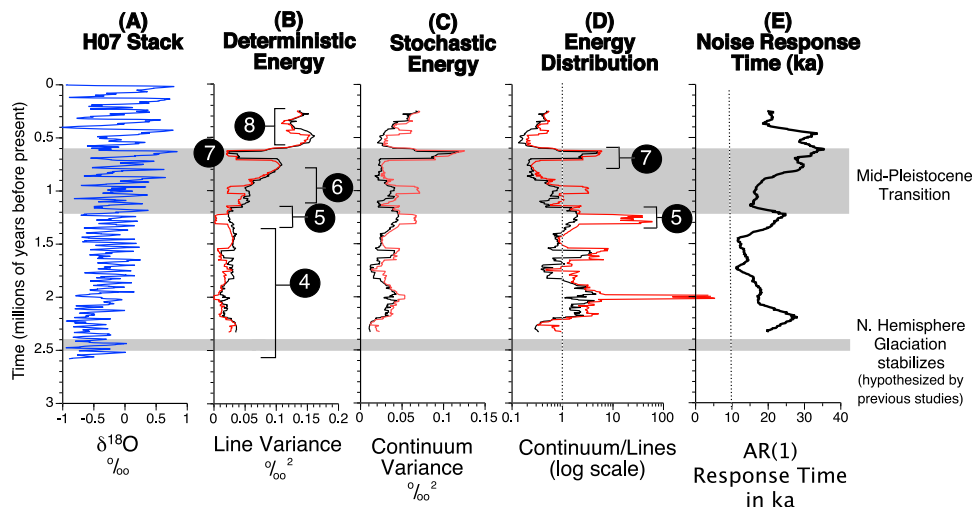


Figure 7. Analysis of the deterministic and stochastic components of climate in the H07 planktic/benthic foraminifera oxygen isotopic stack. (a) The H07 stack. Following the convention of *Huybers* [2007], the mean $\delta^{18}\text{O}$ value between 700 and 0 ka is removed. (b) Evolution of the deterministic line energy observed in the H07 stack. (c) Evolution of the stochastic energy observed in the H07 stack. (d) The ratio of stochastic to deterministic energy. Values greater than one indicate dominance of stochastic energy. (e) Noise response time as determined from the robust AR(1) noise models in Figure 6d. The “noise time constant,” which represents the e -folding time for noise decorrelation [Bartlett, 1966], has been converted to an equivalent climate system response time (the time required for 50% of the climate response to be observed). The black lines in Figures 7b, 7c, and 7d were determined using a 90% significance level threshold for the identification of periodic components, and the red lines employ a more conservative 95% significance level.

tion as the LR04 stack (Figure 4e), but are up to 2.8 times larger, with the greatest discrepancy in the oldest portion of the H07 stack. Given the evidence for timescale distortion noted above, which appears to be more pronounced in the older portion of the H07 stack, it is quite possible that the longer persistence of memory in this record is itself an artifact of timescale error.

5. Discussion and Conclusions

[30] The results of this study reveal that Plio-Pleistocene paleoclimate variability is a complex interplay between deterministic and stochastic climate change. Pleistocene climate is primarily controlled by deterministic climate processes [Shackleton, 2000; Meyers *et al.*, 2008], but also includes intervals during which stochastic elements are of equal or greater importance, as previously suggested by Wunsch [2003, 2004]. Climate noise is more pronounced in the Pliocene, prior to the development of large Northern Hemisphere ice sheets.

[31] The long-term trend of increasing deterministic orbital influence on climate is primarily accommodated during two transitory phases of Northern Hemisphere ice sheet growth. Importantly, these results support an early onset of Northern Hemisphere glaciation at ~ 3.7 Ma [Kleiven *et al.*, 2002; Mudelsee and Raymo, 2005], with exponentially increasing growth until stabilization by ~ 2.6 Ma. This result differs from the more commonly inferred onset at 2.5–2.7 Ma [Shackleton *et al.*, 1984; Haug

et al., 1999; Raymo, 1994; Bintanja and van de Wal, 2008]. Relevant to this issue, precise identification of the onset is complicated by the fact that small transient Northern Hemisphere ice sheets may have been a common feature of the Miocene and Pliocene [Helland and Holmes, 1997; Krissek, 1995; Tripati *et al.*, 2008; DeConto *et al.*, 2008]. Furthermore, the small ice volume signals characteristic of incipient Northern Hemisphere glaciation can be obscured in the benthic $\delta^{18}\text{O}$ record by changes in deep ocean temperature, as well as by dynamics of the Southern Hemisphere ice sheets. These challenges are overcome by partitioning the climate variance into deterministic and stochastic components, which allows us to more clearly resolve subtle isotopic contributions from deterministic periodic control of the ice sheets. Evaluation of noise response time further supports our conclusions, demarcating a period of active ice sheet growth from ~ 3.5 Ma to ~ 2.6 Ma [also see Mudelsee and Raymo, 2005]. Evolution of the Plio-Pleistocene noise response time further suggests that the relative contributions of ice volume and deep ocean temperature to the benthic $\delta^{18}\text{O}$ signal are variable, with a stronger ice volume component imparted when ice sheets are undergoing major long-term expansions. Future research will investigate the use of noise response time to explicitly deconvolve ice volume and deep ocean temperature components of the benthic foraminifera $\delta^{18}\text{O}$ signal.

[32] Superposed on this long-term Plio-Pleistocene trend are transient stochastic events. We interpret these events as evidence for abrupt reorganization of the climate system as

it enters and exits the mid-Pleistocene transition, and at the onset of Northern Hemisphere glaciation. This result is important because it suggests that deterministic orbital influence on climate change is unstable during the initiation and termination of prolonged transitional climate states. However, the precise geophysical mechanism by which such stochastic events arise within the climate system requires further investigation. The dramatic loss of phase coherence associated with these events may ultimately derive from nonlinearities in ice sheet dynamics, thermohaline circulation, and/or the carbon cycle.

[33] Although not the primary purpose of this study, the observation of high amplitude 100 ka and 400 ka $\delta^{18}\text{O}$ cycles during their respective theoretical eccentricity nodes (~ 2.75 Ma and ~ 3.5 Ma) is intriguing. It should be noted that *Lisiecki and Raymo* [2007] have independently observed the same ~ 100 ka cyclic climate variability documented at ~ 2.75 Ma using a different methodology [see *Lisiecki and Raymo*, 2007, Figure 2], but they did not explicitly link it with a short eccentricity node. A range of possible mechanisms for the connection between eccentricity nodes and the emergence of low-frequency climate variability remain to be tested, such as the amplitude and frequency modulating effects of eccentricity on precession [Raymo, 1997], including potential phase locking with the orbital perturbations [Huybers and Wunsch, 2005; Huybers, 2007; Lourens and Hilgen, 1997]. Relevant to this issue, *Bintanja and van de Wal* [2008] propose that the gradual development of a 100,000 year cycle in the late Pleistocene is due to an increase in the ability of North American ice sheets to persist through periodic insolation maxima, itself a consequence of ever greater volumes of ice [see also Raymo, 1997; Berger et al., 1999]. As precession-driven insolation maxima are modulated by eccentricity, it might also be expected that waning short eccentricity variability, as observed in the LA04 orbital solution during the late Pleistocene (Figure 1d), could have promoted the development of the 100,000 year cycle. The emergence of a 100,000 year $\delta^{18}\text{O}$ cycle in the LR04 stack during a short eccentricity node at ~ 2.75 Ma supports this latter hypothesis (Figures 1c, 1d, 2a, and 2b). Furthermore, the emergence of a 400,000 year $\delta^{18}\text{O}$ cycle during a long eccentricity node at ~ 3.5 Ma (Figures 1c, 1d, 2c, and 2d) begs a fundamental role for eccentricity-related changes in fostering long-period glacial cycles, most likely via its influence on precession-driven insolation maxima [e.g., see Raymo, 1997].

[34] The absence of LR04 “eccentricity band” climate variability associated with LA04 eccentricity nodes at 4.75 Ma and 1.4 Ma (Figure 1d), indicates that the mere existence of this particular orbital configuration is not sufficient to explain the observed long-period climate variability. For example, the absence of 100 ka cyclic climate variance at 4.75 Ma is likely due to the fact that this

eccentricity node predates the formation of the Isthmus of Panama, which is believed to be a critical factor for the emergence of large scale Northern Hemisphere glaciation [Haug and Tiedemann, 1998]. This highlights the importance of interactions between orbital insolation influences and long-term changes in Earth’s mean climate state. Our results suggest that eccentricity modulations indirectly precondition for the development of long-period climate variability in the Northern Hemisphere ice sheets by altering (diminishing) precession-related insolation maxima, and thus increase the likelihood for persistence of ice sheets through multiple insolation maxima. However, long-period climate variability is only manifested if the growth of ice sheets is otherwise favorable. With respect to this issue, it is important to note that although long-period climate variance appears to be promoted by the presence of the insolation nodes, the precise geophysical mechanism responsible for the 100,000 year and 400,000 year pacing of the glacial cycles that emerge is uncertain. Potential candidates for this pacing include cyrosphere and carbon cycle dynamics [e.g., Clark et al., 1999; Ruddiman, 2003; Tziperman and Gildore, 2003; Rial, 2004; Huybers and Wunsch, 2005].

[35] Comparison of results from the analysis of the LR04 and H07 stacks reveal many similarities, and a consistent interpretation in climate system evolution. However, an important distinction between the two records is the degradation of phase coherence in portions of the H07 stack, resulting in a general increase in the stochastic contribution. Multiple lines of evidence suggest that this degradation of phase coherence, which becomes pronounced in the early Pleistocene, is attributable to timescale error. For example, at least two of the stochastic events observed in the H07 stack (absent in the LR04 stack) are potentially artifacts of timescale distortion, related to sedimentation rate changes that are paced by long eccentricity. These are topics that require further scrutiny.

[36] Future work will investigate the sources of noise that are observed in the LR04 and H07 stacks, and address the physical mechanisms responsible for the abrupt climate reorganization events. Importantly, the results from this study provide objective targets for future climate modeling studies; characterization of the spectral continuum and the orbital lines provide a “fingerprint” of the climate system response, which in combination with climate modeling studies, can be used to test competing hypotheses for the cause(s) of the observed climate change.

[37] **Acknowledgments.** The authors wish to express thanks to Jeffery Park, Gerald Dickens, and an anonymous reviewer for thoughtful comments that substantially improved this manuscript. S.R.M. thanks Lorraine Lisiecki for insightful discussion pertaining to the LR04 stack.

References

- Bartlett, M. S. (1966), *An Introduction to Stochastic Processes*, 362 pp., Cambridge Univ. Press, Cambridge, U. K.
- Benzi, R., G. Parisi, A. Sutera, and A. Vulpiani (1983), A theory of stochastic resonance in climatic change, *SIAM J. Appl. Math.*, *43*, 565–578, doi:10.1137/0143037.
- Berger, A., X. S. Li, and M. F. Loutre (1999), Modelling Northern Hemisphere ice volume over the last 3 Ma, *Quat. Sci. Rev.*, *18*, 1–11, doi:10.1016/S0277-3791(98)00033-X.
- Berner, R. A., and Z. Kothavala (2001), GEOCARB III: A revised model of atmospheric CO_2 over

- Phanerozoic time, *Am. J. Sci.*, 301, 182–204, doi:10.2475/ajs.301.2.182.
- Bintanja, R., and R. S. W. van de Wal (2008), North American ice-sheet dynamics and the onset of 100,000-year glacial cycles, *Nature*, 454, 869–872, doi:10.1038/nature07158.
- Cane, M. A., and P. Molnar (2001), Closing of the Indonesian seaway as a precursor to East African aridification around 3–4 million years ago, *Nature*, 411, 157–162, doi:10.1038/35075500.
- Clark, P. U., and D. Pollard (1998), Origin of the middle Pleistocene transition by ice sheet erosion of regolith, *Paleoceanography*, 13, 1–9, doi:10.1029/97PA02660.
- Clark, P. U., R. B. Alley, and D. Pollard (1999), Northern Hemisphere ice-sheet influences on global climate change, *Science*, 286, 1104–1111, doi:10.1126/science.286.5442.1104.
- Clark, P. U., D. Archer, D. Pollard, J. D. Blum, J. A. Rial, V. Brovkin, A. Mix, N. G. Pisias, and M. Roy (2006), The middle Pleistocene transition: Characteristics, mechanisms, and implications for long-term changes in atmospheric pCO₂, *Quat. Sci. Rev.*, 25, 3150–3184, doi:10.1016/j.quascirev.2006.07.008.
- DeConto, R. M., D. Pollard, P. A. Wilson, H. Palike, H. Lear, and M. Pagani (2008), Thresholds for Cenozoic bipolar glaciation, *Nature*, 455, 652–656, doi:10.1038/nature07337.
- Ditlevsen, P. D. (2009), Bifurcation structure and noise-assisted transitions in the Pleistocene glacial cycles, *Paleoceanography*, 24, PA3204, doi:10.1029/2008PA001673.
- Ganopolski, A., and S. Rahmstorf (2002), Abrupt glacial climate changes due to stochastic resonance, *Phys. Rev. Lett.*, 88, 038501, doi:10.1103/PhysRevLett.88.038501.
- Hasselmann, K. (1976), Stochastic climate models: Part I. Theory, *Tellus*, 28, 473–485, doi:10.1111/j.2153-3490.1976.tb00696.x.
- Haug, G. H., and R. Tiedemann (1998), Effect of the formation of the Isthmus of Panama on Atlantic Ocean thermohaline circulation, *Nature*, 393, 673–676, doi:10.1038/31447.
- Haug, G. H., D. M. Sigman, R. Tiedemann, T. F. Pedersen, and M. Sarnthein (1999), Onset of permanent stratification in the subarctic Pacific Ocean, *Nature*, 401, 779–782, doi:10.1038/44550.
- Hays, J. D., J. Imbrie, and N. J. Shackleton (1976), Variations in the Earth's orbit: Pacemaker of the ice ages, *Science*, 194, 1121–1132, doi:10.1126/science.194.4270.1121.
- Helland, P. E., and M. A. Holmes (1997), Surface textural analysis of quartz sand grains from ODP Site 918 off the southeast coast of Greenland suggests glaciation of southern Greenland at 11 Ma, *Palaeoogeogr. Palaeoecol.*, 135, 109–121, doi:10.1016/S0031-0182(97)00025-4.
- Herbert, T. (1997), A long marine history of carbon cycle modulation by orbital-climatic changes, *Proc. Natl. Acad. Sci. U. S. A.*, 94, 8362–8369, doi:10.1073/pnas.94.16.8362.
- Hinnov, L. A. (2000), New perspectives on orbitally forced stratigraphy, *Annu. Rev. Earth Planet. Sci.*, 28, 419–475, doi:10.1146/annurev.earth.28.1.419.
- Hönisch, B., N. G. Hemming, D. Archer, M. Siddall, and J. F. McManus (2009), Atmospheric carbon dioxide concentration across the mid-Pleistocene transition, *Science*, 324, 1551–1554, doi:10.1126/science.1171477.
- Huybers, P. (2007), Glacial variability over the last 2 Ma: An extended depth-derived age model, continuous obliquity pacing, and the Pleistocene progression, *Quat. Sci. Rev.*, 26, 37–55, doi:10.1016/j.quascirev.2006.07.013.
- Huybers, P., and W. Curry (2006), Links between annual, Milankovitch and continuum temperature variability, *Nature*, 441, 329–332, doi:10.1038/nature04745.
- Huybers, P., and C. Wunsch (2004), A depth-derived Pleistocene age model: Uncertainty estimates, sedimentation variability, and non-linear climate change, *Paleoceanography*, 19, PA1028, doi:10.1029/2002PA000857.
- Huybers, P., and C. Wunsch (2005), Obliquity pacing of the late Pleistocene glacial terminations, *Nature*, 434, 491–494, doi:10.1038/nature03401.
- Imbrie, J., and J. Z. Imbrie (1980), Modeling the climatic response to orbital variations, *Science*, 207, 943–953, doi:10.1126/science.207.4434.943.
- Imbrie, J., et al. (1992), On the structure and origin of major glaciation cycles: 1. Linear responses to Milankovitch forcing, *Paleoceanography*, 7, 701–738, doi:10.1029/92PA02253.
- Imbrie, J., et al. (1993), On the structure and origin of major glaciation cycles: 2. The 100,000-year cycle, *Paleoceanography*, 8, 699–735, doi:10.1029/93PA02751.
- Keigwin, L. (1982), Isotopic paleoceanography of the Caribbean and East Pacific: Role of Panama uplift in late Neogene time, *Science*, 217, 350–353, doi:10.1126/science.217.4557.350.
- Kleiven, H. F., E. Jansen, T. Fronval, and T. M. Smith (2002), Intensification of Northern Hemisphere glaciations in the circum Atlantic region (3.5–2.4 Ma)—Ice-rafted detritus evidence, *Palaeoogeogr. Palaeoecol.*, 184, 213–223, doi:10.1016/S0031-0182(01)00407-2.
- Kominz, M. A., and N. G. Pisias (1979), Pleistocene climate: Deterministic or stochastic?, *Science*, 204, 171–173, doi:10.1126/science.204.4389.171.
- Krissek, L. A. (1995), Late Cenozoic ice-rafting records from Leg 145 sites in the North Pacific: Late Miocene onset, late Pliocene intensification, and Plio-Pleistocene events, *Proc. Ocean Drill. Program Sci. Results*, 145, 179–194.
- Laskar, J., P. Robutel, F. Joutel, M. Gastineau, A. C. M. Correia, and B. Levard (2004), A long-term numerical solution for the insolation quantities of the Earth, *Astron. Astrophys.*, 428, 261–285, doi:10.1051/0004-6361:20041335.
- Lawver, L. A., and L. M. Gahagan (2003), Evolution of Cenozoic seaways in the circum-Antarctic region, *Palaeoogeogr. Palaeoecol.*, 198, 11–37, doi:10.1016/S0031-0182(03)00392-4.
- Lisiecki, L. E., and M. E. Raymo (2005), A Pliocene-Pleistocene stack of 57 globally distributed benthic $\delta^{18}\text{O}$ records, *Paleoceanography*, 20, PA1003, doi:10.1029/2004PA001071.
- Lisiecki, L. E., and M. E. Raymo (2007), Plio-Pleistocene climate evolution: Trends and transitions in glacial cycle dynamics, *Quat. Sci. Rev.*, 26, 56–69, doi:10.1016/j.quascirev.2006.09.005.
- Lorenz, E. N. (1976), Nondeterministic theories of climate change, *Quat. Res.*, 6, 495–506, doi:10.1016/0033-5894(76)90022-3.
- Lourens, L. J., and F. J. Hilgen (1997), Long-periodic variations in the Earth's obliquity and their relationship to third-order eustatic cycles and late Neogene glaciations, *Quat. Int.*, 40, 43–52, doi:10.1016/S1040-6182(96)00060-2.
- Lourens, L. J., A. Sluijs, D. Kroon, J. C. Zachos, E. Thomas, U. Röhl, J. Bowles, and I. Raffi (2005), Astronomical pacing of late Palaeocene to early Eocene global warming events, *Nature*, 435, 1083–1087, doi:10.1038/nature03814.
- Mann, M. E., and J. M. Lees (1996), Robust estimation of background noise and signal detection in climatic time series, *Clim. Change*, 33, 409–445, doi:10.1007/BF00142586.
- Meyers, S. R., B. B. Sageman, and L. A. Hinnov (2001), Integrated quantitative stratigraphy of the Cenomanian-Turonian Bridge Creek limestone member using evolutive harmonic analysis and stratigraphic modeling, *J. Sediment. Res.*, 71, 628–644, doi:10.1306/012401710628.
- Meyers, S. R., B. B. Sageman, and M. Pagani (2008), Resolving Milankovitch: Consideration of signal and noise, *Am. J. Sci.*, 308, 770–786, doi:10.2475/06.2008.02.
- Milankovitch, M. (1941), *Kanon der Erdbestrahlung und Seine Anwendung auf das Eiszeitenproblem*, 633 pp., K. Serbische Akad., Belgrade.
- Mitchell, J. M. (1976), An overview of climatic variability and its causal mechanisms, *Quat. Res.*, 6, 481–493, doi:10.1016/0033-5894(76)90021-1.
- Mudelsee, M., and M. E. Raymo (2005), Slow dynamics of the Northern Hemisphere glaciation, *Paleoceanography*, 20, PA4022, doi:10.1029/2005PA001153.
- Pagani, M., J. C. Zachos, K. H. Freeman, B. Tipler, and S. Bohaty (2005), Marked decline in atmospheric carbon dioxide concentrations during the Paleogene, *Science*, 309, 600–603, doi:10.1126/science.1110063.
- Pälike, H., and F. Hilgen (2008), Rock clock synchronization, *Nat. Geosci.*, 1, 282, doi:10.1038/ngeo197.
- Pälike, H., R. Norris, J. O. Herrle, P. Wilson, H. K. Coxall, C. H. Lear, N. J. Shackleton, A. K. Tripathi, and B. S. Wade (2006), The heartbeat of the Oligocene climate system, *Science*, 314, 1894–1898, doi:10.1126/science.1133822.
- Park, J., and T. D. Herbert (1987), Hunting for paleoclimatic periodicities in a geologic time series with an uncertain time scale, *J. Geophys. Res.*, 92, 14,027–14,040, doi:10.1029/JB092iB13p14027.
- Pearson, P. N., and M. R. Palmer (2000), Atmospheric carbon dioxide concentrations over the past 60 million years, *Nature*, 406, 695–699.
- Pelletier, J. D. (1998), The power spectral density of atmospheric temperature from time scales of 10² to 10⁶ yr, *Earth Planet. Sci. Lett.*, 158, 157–164, doi:10.1016/S0012-821X(98)00051-X.
- Pelletier, J. D. (2002), Natural variability of atmospheric temperature and geomagnetic intensity over a wide range of time scales, *Proc. Natl. Acad. Sci. U. S. A.*, 99, 2546–2553, doi:10.1073/pnas.022582599.
- Pelletier, J. D. (2003), Coherence resonance and ice ages, *J. Geophys. Res.*, 108(D20), 4645, doi:10.1029/2002JD003120.
- Pelletier, J. D., and D. L. Turcotte (1997), Long-range persistence in climatological and hydrological time series: Analysis, modeling and application to drought hazard assessment, *J. Hydrol.*, 203, 198–208.
- Percival, D. B., and A. T. Walden (1993), *Spectral Analysis for Physical Applications*, 583 pp., doi:10.1017/CBO9780511622762, Cambridge Univ. Press, Cambridge, U. K.

- Raymo, M. E. (1994), The initiation of Northern Hemisphere glaciation, *Annu. Rev. Earth Planet. Sci.*, **22**, 353–383, doi:10.1146/annurev.ea.22.050194.002033.
- Raymo, M. E. (1997), The timing of major climate terminations, *Paleoceanography*, **12**, 577–585, doi:10.1029/97PA01169.
- Rial, J. A. (2004), Abrupt climate change: Chaos and order at orbital and millennial scales, *Global Planet. Change*, **41**, 95–109, doi:10.1016/j.gloplacha.2003.10.004.
- Royer, D. L. (2006), CO₂-forced climate thresholds during the Phanerozoic, *Geochim. Cosmochim. Acta*, **70**, 5665–5675, doi:10.1016/j.gca.2005.11.031.
- Ruddiman, W. F. (2003), Orbital insolation, ice volume, and greenhouse gases, *Quat. Sci. Rev.*, **22**, 1597–1629, doi:10.1016/S0277-3791(03)00087-8.
- Saltzman, B. (1982), Stochastically driven climatic fluctuations in the sea-ice, ocean temperature, CO₂ feedback system, *Tellus*, **34**, 97–112, doi:10.1111/j.2153-3490.1982.tb01797.x.
- Shackleton, N. J. (2000), The 100,000-year ice-age cycle identified and found to lag temperature, carbon dioxide, and orbital eccentricity, *Science*, **289**, 1897–1902, doi:10.1126/science.289.5486.1897.
- Shackleton, N. J., et al. (1984), Oxygen isotope calibration of the onset of ice-rafting and history of glaciation in the North Atlantic region, *Nature*, **307**, 620–623, doi:10.1038/307620a0.
- Thomson, D. J. (1982), Spectrum estimation and harmonic analysis, *Proc. IEEE*, **70**, 1055–1096, doi:10.1109/PROC.1982.12433.
- Tripati, A. K., et al. (2008), Evidence for glaciation in the Northern Hemisphere back to 44 Ma from ice-rafted debris in the Greenland Sea, *Earth Planet. Sci. Lett.*, **265**, 112–122, doi:10.1016/j.epsl.2007.09.045.
- Tziperman, E., and H. Gildore (2003), On the mid-Pleistocene transition to 100-kyr glacial cycles and the asymmetry between glaciation and deglaciation times, *Paleoceanography*, **18**(1), 1001, doi:10.1029/2001PA000627.
- Wunsch, C. (2003), The spectral description of climate change including the 100 ky energy, *Clim. Dyn.*, **20**, 353–363.
- Wunsch, C. (2004), Quantitative estimate of the Milankovitch-forced contribution to observed Quaternary climate change, *Quat. Sci. Rev.*, **23**, 1001–1012, doi:10.1016/j.quascirev.2004.02.014.
- Yiou, P., C. Genthon, M. Ghil, J. Jouzel, H. Le Treut, J. M. Barnola, C. Lorius, and Y. N. Korotkevitch (1991), High-frequency paleovariability in climate and CO₂ levels from Vostok ice core records, *J. Geophys. Res.*, **96**, 20,365–20,378, doi:10.1029/91JB00422.
- Zachos, J., M. Pagani, L. Sloan, E. Thomas, and K. Billups (2001), Trends, rhythms, and aberrations in global climate 65 Ma to present, *Science*, **292**, 686–693, doi:10.1126/science.1059412.

L. A. Hinnov, Morton K. Blaustein Department of Earth and Planetary Sciences, Johns Hopkins University, Baltimore, MD 21218, USA. (hinnov@jhu.edu)

S. R. Meyers, Department of Geoscience, University of Wisconsin-Madison, Madison, WI 53706, USA. (smeyers@geology.wisc.edu)

LR04 Stack Evolutive Harmonic Analysis Amplitudes Normalized

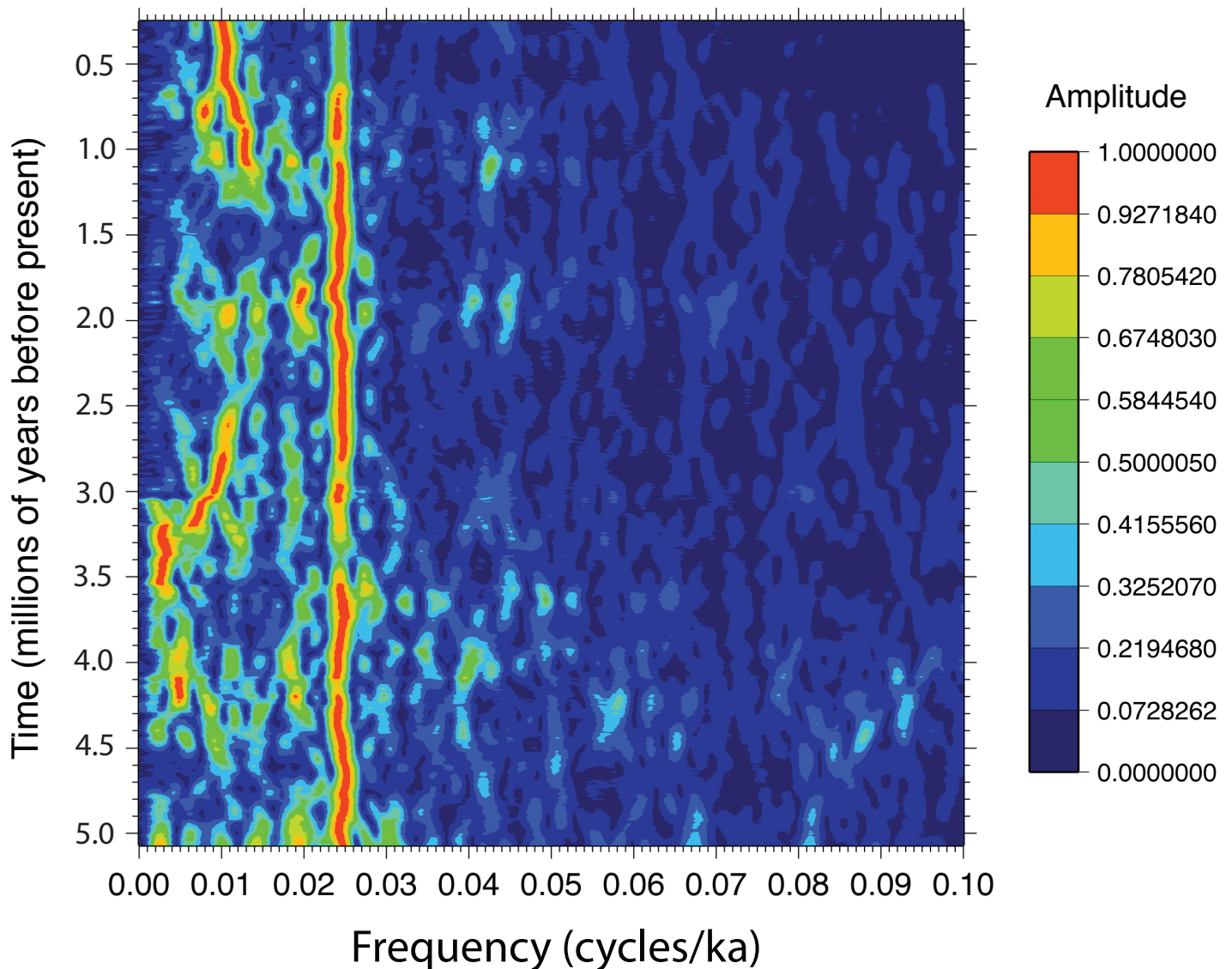


Figure S1. MTM evolutive harmonic analysis results for the LR04 stack. All EHA computations were conducted using three 2π prolate tapers, and a 500 ka moving window with a 5 ka increment. The mean value and a linear trend have been removed from each 500 ka data window prior to analysis. In this figure, the EHA amplitude results in Figure 1B are normalized so that each individual spectrum has a maximum amplitude of unity.